White Matter Fiber-Bundle Analysis Using Non-negative Tensor Factorization

Claudio Stamile[1,2], François Cotton[1,4], Frederik Maes[3], Dominique Sappey-Marinier[1,5], and Sabine Van Huffel[2,6(✉)]

[1] CREATIS, CNRS UMR5220, INSERM U1044, Université de Lyon, Université Lyon 1, INSA-Lyon, Lyon, France
stamile@creatis.insa-lyon.fr
[2] Department of Electrical Engineering (ESAT), STADIUS, KU Leuven, Leuven, Belgium
Sabine.VanHuffel@esat.kuleuven.be
[3] Department of Electrical Engineering (ESAT), PSI, KU Leuven, Leuven, Belgium
[4] Service de Radiologie, Centre Hospitalier Lyon-Sud, Hospices Civils de Lyon, Pierre-Bénite, France
[5] CERMEP - Imagerie du Vivant, Université de Lyon, Bron, France
[6] iMinds Medical Information Technologies, Leuven, Belgium

Abstract. With the development of advanced image acquisition and processing techniques providing better biomarkers for the characterization of brain diseases, the automatic analysis of biomedical imaging constitutes a critical point. In particular, analysis of complex data structure is a challenge for better understanding complex brain pathologies like multiple sclerosis (MS).

In this work, we describe a new fully automated method based on non-negative tensor factorization (NTF) to analyze white matter (WM) fiber-bundles. This method allows to extract, from a WM fiber-bundle, the set of fibers affected by the pathology, discriminating fibers affected by the pathological from the healthy fibers.

Our method was validated on simulated data and also applied on real MS patients. Results show the high precision level of our method to extract fibers affected by the pathological process.

Keywords: Non-negative tensor factorization · White matter · Multiple sclerosis · DTI · Tractography

1 Introduction

In the last decade, the interest in new methods to analyze white matter (WM) fiber-bundles increased. Different papers [3,7,14] suggest how the analysis of WM structures using diffusion tensor imaging (DTI) information is a powerful tool to better investigate neurodegenerative processes. All those methods were largely applied to characterize WM structure affected by the pathology [3,7] and also to understand the brain development mechanisms [14].

© Springer International Publishing Switzerland 2016
A. Campilho and F. Karray (Eds.): ICIAR 2016, LNCS 9730, pp. 650–657, 2016.
DOI: 10.1007/978-3-319-41501-7_73

From a methodological point of view, all these techniques present different limitations. In [3,7] the authors show a first semi-automated method to analyze the mean signal profile along the WM structure. Unfortunately both methods are not fully automated, in particular, the extraction of the fiber-bundles of interest should be performed manually by a neurologist. This manual step drastically reduces the possibility to apply the method to large datasets. A first example of a fully automated method is described in [14]. In this paper the authors described a pipeline that allows to extract and study how the signal changes along different WM fiber-bundles. If the method performs a fully automated analysis, it still analyzes the mean signal profile of the fiber-bundle. The simple mean analysis of the signal reduces the sensitivity of the method to detect the presence of "abnormal" regions [10] especially when those changes are relatively small like relapsing remitting (RR) form of multiple sclerosis (MS). Furthermore, this approach does not allow to distinguish which set of fibers within the bundle are affected by the pathology and which are not. As ulterior point, all the methods previously described do not allow to analyze multiple diffusion maps at the same time, reducing the capability to exploit complementary information.

In order to overcome all these limitations, in this paper a new fully automated method is presented. Major contribution is given by the original application of non-negative tensor factorization (NTF) to analyze WM fiber-bundles. Compared to the other techniques, NTF allows to have a global view of the fiber-bundle allowing to better characterize the subset of fibers affected by the pathology. Moreover, due to the adaptability of NTF, complementary information derived from multiple diffusion maps could be used at the same time.

Tests on simulated and real data show the capability of our method to distinguish between fibers affected by the pathological process and fibers belonging to normal tissue.

This paper is structured as follows. In Sect. 2, we provide a detailed description of our approach. In Sect. 3, we present our experimental campaign. Finally, in Sect. 4, we draw our conclusions.

2 Materials and Methods

2.1 Data Acquisition and Protocol

Five relapsing-remitting (RR) MS patients (4 women and 1 man, mean ($\pm$SD) age: 36.8 ± 9.5 years; media disease duration: 4.24y; max 16.5y) (median Expanded Disability Status Scale (EDSS) = 2.5, range = [0; 4]) and one healthy control (HC) subject (age: 24y) were included in this study. Inclusion criteria specified that studied patients were diagnosed as RR MS if they present at least one new Gadolinium-enhancing lesion during the six months preceding study enrollment. The DTI image set consisted of the acquisition of 60 contiguous 2 mm-thick slices parallel to the bi-commissural plane (AC-PC), and were acquired using a 2D Echo-Planar Imaging (EPI) sequence (TE/TR = 60/8210 ms, FOV = $224 \times 224 \times 120\,\text{mm}^3$) with 32 gradient directions ($b = 1000\ \frac{s}{mm^2}$). The nominal voxel size at acquisition ($2 \times 2 \times 2\,\text{mm}^3$) was interpolated to $0.875 \times 0.875 \times 2\,\text{mm}^3$ after reconstruction.

2.2 Processing and Fiber-Bundle Extraction

Diffusion data of each subject are processed in order to compute the tensor model using the FDT module of FSL. The obtained tensor image is then non-rigidly co-registered to the Illinois Institute of Technology (IIT) atlas [13] using the DTI ToolKit (DTI-TK) [15]. The resulting tensor image is then used to compute 6 diffusion metric maps: fractional anisotropy (FA), mean diffusivity (MD), radial diffusivity (λ_r) and the three eigenvalues of diffusion tensor (λ_1, λ_2, λ_3). Probabilistic streamline tractography was performed using MRTrix [12] based on the fiber orientation density (FOD) information of IIT Atlas. From the atlas, twenty fiber bundles were extracted using 20 ROIs of the JHU atlas [5] as seed and mask. Fibers within each of the 20 bundles are then reordered according to common start/end point. For each fiber-bundle, a classical K-Means algorithm [6] is performed to generate two different clusters, R_1 for the starting points and R_2 for the ending points. Fiber points are then reordered from R_1 to R_2 and fibers that did not link the two clusters (broken fibers) are automatically removed. As final post-processing step each fiber is resampled with the same number $c = 100$ of points (also called nodes). Fiber-bundles processed with the previous described pipeline could be formalized as a set $Z = \{f_1, f_2, \ldots, f_n\}$ composed of n fibers $f_i = \{p_1, \ldots, p_c\}$ where $p_q = (x_q, y_q, z_q) \mid 1 \leq q \leq c$. The coordinate p_q is used to extract the voxel's value of one of the m diffusion maps in the corresponding location of f_i. With this formalization it is possible to analyze the changes of each diffusion map along each fiber belonging to a bundle.

2.3 Tensor Construction

Application of a tensor model to analyze brain data is a recent trend in signal processing. More in detail, a tensor model was successfully applied to event related potential (ERP) analysis [16] but also to tumor tissue type differentiation based on magnetic resonance spectroscopic imaging [4]. In this work tensor factorization is applied on diffusion data.

Starting from a fiber-bundle we create a tensor $\mathcal{X} \in \mathbb{R}^{c \times n \times m}$ (Fig. 1). Where c is the number of cross-sections of each fiber, n is the number of fibers within the bundle and m is the number of diffusion maps that we want to use. Following this tensor formalization, an element $x_{i,j,k} \in \mathcal{X}$ represents the value in the $i-th$ cross-section of the $j-th$ fiber of the bundle, extracted from the $k-th$ modality. This tensor formalization give us the possibility to analyze, at the same time, local and global aspects of a fiber-bundle. Local information could be obtained by analyzing $x_{:,j,k}$ which represents the values of the $k-th$ modality extracted along all the cross-sections of the $j-th$ fiber. We can also obtain global information of the fiber-bundle by analyzing $x_{i,:,k}$ which represents the values on the entire $i-th$ cross-section extracted from the $k-th$ modality (Fig. 1).

With this formalization it is easy to see how cross-section based methods, like the two described in [10,11], are special cases of the tensor-based model. In this paper we use C to denote the cross-sectional component, F to denote the

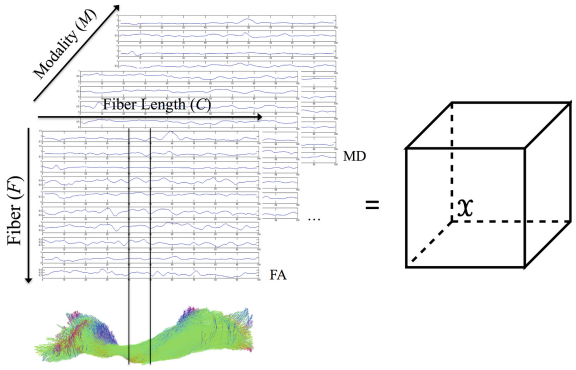


Fig. 1. Tensor representation of WM fiber-bundle

fiber-wise component and M to denote the modality component of the tensor $\mathcal{X}$ representing a fiber-bundle.

2.4 Non-negative CPD Analysis

The non-negative canonical polyadic decomposition (NCPD) decomposition factorizes [2] a tensor into a sum of positive component rank-one tensors. For example, given a third-order tensor $\mathcal{T} \in \mathbb{R}^{i \times j \times k}$ we wish to write it as:

$$\mathcal{T} \approx [\![ABC]\!] = \sum_{r=1}^{R} a_r \circ b_r \circ c_r \qquad A, B, C \geq 0 \tag{1}$$

where $A = [a_1, \ldots, a_R] \in \mathbb{R}_+^{i \times R}$, $B = [b_1, \ldots, b_R] \in \mathbb{R}_+^{j \times R}$, $C = [c_1, \ldots, c_R] \in \mathbb{R}_+^{k \times R}$ are non-negative factor matrices. R is the rank, defined as the number of rank-one terms and "$\circ$" represent the outer product.

In our case, in order to compute the CPD of the tensor $\mathcal{X}$ built starting from a fiber-bundle, the solution of the following optimization problem is required:

$$[C^*, F^*, M^*] = \min_{C,F,M \geq 0} \left\| \mathcal{X} - \sum_{i=1}^{R} C(:,i) \circ F(:,i) \circ M(:,i) \right\|_2^2 + \alpha \|Vec(F)\|_1 \tag{2}$$

where C, F and M are the aftermentioned cross-section, fibers and modality matrices and α is the parameter that control the sparsity imposed by using l_1-norm regularization. In this work the optimization problem 2 with non-negativity constraints is solved using the structured data fusion method [9] available in Tensorlab [8]. As last step, in order to associate at each fiber one of the three classes of tissues, the k-means++ algorithm [1] is applied on the fiber component (F^*) obtained from the NCPD.

3 Experiments

3.1 Simulated Data

30 different "pathological" variations were simulated on the control subject's diffusion maps. All the variations were generated along 3 different fiber-bundles, namely, cortico-spinal tract (CST), superior longitudinal fasciculi (SLF), and inferior longitudinal fasciculi (IFO). Small spherical regions of radius r were randomly selected along the WM fiber-bundles. The voxel's eigenvalues inside each region were changed according to the following equations:

$$\lambda_2^* = \lambda_2 + \rho * (\lambda_1 - \lambda_2) \quad \lambda_3^* = \lambda_3 + \rho * (\lambda_1 - \lambda_3)$$

and all diffusion metrics were recomputed according to the new value of λ_2^* and λ_3^*. In order to simulate small variations, we performed the tests using $r = 2$ and $\rho = 0.2$. Along each fiber-bundle 2 or 3 regions were randomly selected to put the signal changes. To quantify the quality of the delineation of the fibers containing the simulated variations, the True Positive (TP), True Negative (TN), False Positive (FP) and False Negative (FN) fractions were used to compute the performance measurements used in this work. More in detail we focus our attention on the precision ($P_r = \frac{TP}{TP+FP}$), recall ($R_e = \frac{TP}{TP+FN}$) and F-Measure ($M_e = \frac{2*TP}{2*TP+FP+FN}$). Since multiple test were performed, for each of the three diffusion metrics, mean ($\overline{P_r}$, $\overline{R_e}$, $\overline{M_e}$) and standard deviation (σP_r, σR_e, σM_e) were computed.

Rank of $R = 3$ was selected for NCPD. This value was chosen based on the presence of 3 main regions: *(i)* healthy tissue, *(ii)* "pathological" tissue, *(iii)* voxels with partial volume effect. Automatic rank selection is still an open problem and needs to be explored through further research.

Different tests were performed using different diffusion metrics at the same time ("λ_2, λ_3", "$FA, MD, \lambda_2, \lambda_3$" and "$FA, MD$"). Moreover, in order to find the best value of the regularization weight α, tests were performed with different values. The α-interval ($0 < \alpha \leq 0.8$) was divided into 30 steps. We reported the results for certain values of α in Table 1. Best results were obtained using $\alpha = 0.1388$ and using λ_2, λ_3 as features. Worst performances were obtained using $\alpha = 0.6898$ and $\lambda_2, \lambda_3, FA, MD$ as features. We can also see how the regularization parameter α strongly influences the quality of the delineation. Indeed, high values of α show a degradation in the detection performances. Similar behavior is also visible for small values of α. The best results were visible in the range going from $\alpha = 0.0561$ to $\alpha = 0.1939$. Despite the high values of precision, the proposed method shows low performances in term of recall. Indeed, the method seems to underestimate the subset of fibers really affected by the pathological process.

3.2 Application on Multiple Sclerosis Patients

The proposed method was also applied on real data. More in detail, the CST and SLF of two MS subjects from the dataset described in Sect. 2.1 were selected.

Table 1. Changes in mean ($\overline{P_r}$, $\overline{R_e}$, $\overline{M_e}$) and standard deviation (σP_r, σR_e, σM_e) of precision, recall and F-Measure according to regularization parameter (α) and different features.

	λ_2, λ_3						**FA, MD,** λ_2, λ_3						**FA, MD**					
α	$\overline{P_r}$	σP_r	$\overline{R_e}$	σR_e	$\overline{M_s}$	σM_s	$\overline{P_r}$	σP_r	$\overline{R_e}$	σR_e	$\overline{M_s}$	σM_s	$\overline{P_r}$	σP_r	$\overline{R_e}$	σR_e	$\overline{M_s}$	σM_s
0.0561	0.66	0.17	0.48	0.16	0.53	0.15	0.65	0.20	0.38	0.19	0.44	0.18	0.61	0.19	0.39	0.15	0.44	0.13
0.0837	0.66	0.19	0.41	0.18	0.48	0.19	0.69	0.17	0.41	0.22	0.47	0.19	0.61	0.18	0.40	0.09	0.47	0.10
0.1112	0.64	0.19	0.47	0.17	0.51	0.16	0.66	0.16	0.37	0.20	0.43	0.18	0.60	0.18	0.38	0.10	0.45	0.11
0.1388	**0.67**	**0.16**	**0.42**	**0.18**	**0.49**	**0.16**	0.69	0.17	0.40	0.20	0.47	0.18	0.61	0.19	0.39	0.09	0.46	0.09
0.1663	0.67	0.19	0.41	0.20	0.47	0.19	0.68	0.16	0.34	0.21	0.41	0.21	0.60	0.18	0.43	0.10	0.48	0.09
0.1939	0.65	0.19	0.44	0.18	0.50	0.15	0.69	0.18	0.36	0.20	0.44	0.19	0.59	0.18	0.37	0.11	0.44	0.10
0.2490	0.65	0.16	0.35	0.18	0.42	0.18	0.66	0.17	0.37	0.20	0.44	0.19	0.60	0.19	0.36	0.13	0.43	0.11
0.5520	0.67	0.18	0.42	0.16	0.48	0.12	0.63	0.16	0.39	0.24	0.43	0.21	0.60	0.17	0.41	0.18	0.46	0.16
0.6898	0.64	0.16	0.41	0.22	0.46	0.19	0.60	0.18	0.30	0.20	0.34	0.18	0.62	0.18	0.43	0.18	0.47	0.15
0.7449	0.63	0.19	0.37	0.16	0.44	0.17	0.58	0.19	0.42	0.21	0.44	0.19	0.61	0.19	0.37	0.17	0.42	0.15

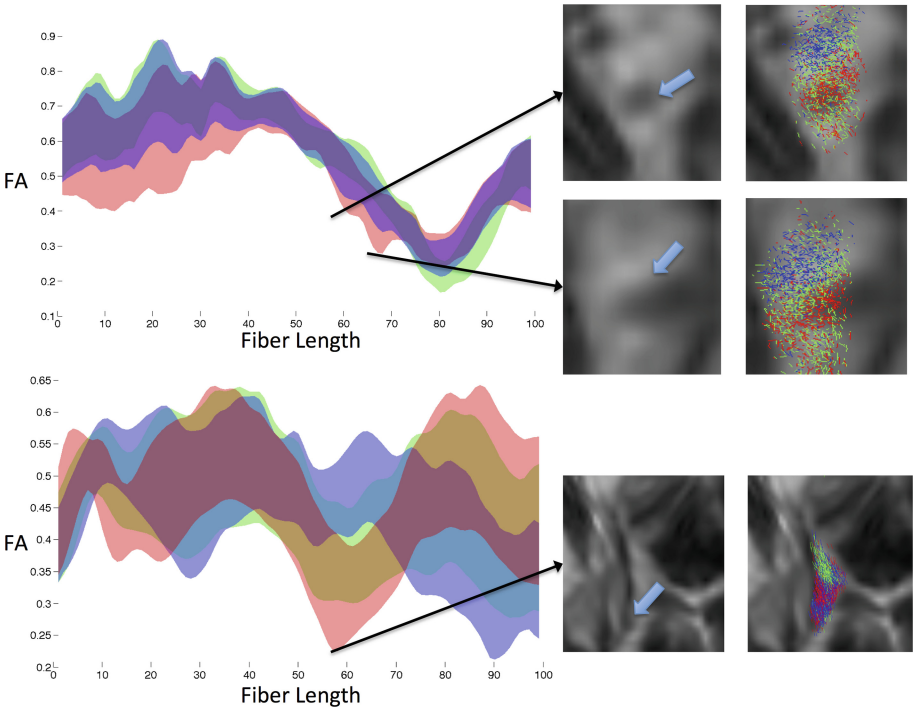


Fig. 2. Application of tensor factorization on two fiber-bundles in two MS patients. On top CST of the first subject. On left, the mean signal profile of FA along each set of fibers shows that the red fibers have change the FA signal in two regions corresponding to MS lesions (right figures). On the bottom plot, the mean FA signal along fibers belonging to SLF on the second MS patient. The red fiber-bundle show a large change in the regions affected by the pathology due to the presence of MS lesion (right figure).

Using the results obtained in the previous section, we used as regularization parameter $\alpha = 0.1388$ and λ_2, λ_3 as features. Results of the application are shown in Fig. 2. The application on the MS patients, shows the capability of our method to detect subsets of fibers within the bundle affected by the pathological event. The quality of the fiber-bundle extraction is also confirmed by the analysis of the mean FA signal [14]. The mean signal profile shows along each subset of fibers, how in certain cross-sections a change in the signal, appears. It is possibile to see how, for one fiber-bundle a negative-peak in the FA signal is present in certain cross-sections. This behavior is not confirmed by the other fiber-bundles. Indeed, for the other two classes of fibers the mean FA profile does not show cross-sections where the signal drastically changes.

4 Conclusion

In this work we described a new fully automated pipeline capable to analyze WM fiber-bundles. The major contribution is the application of NTF to WM analysis. We showed how a tensor-based model is a powerful tool to analyze fiber-bundles taking into account multi diffusion maps information. The capability of our method to distinguish between sets of fibers affected by pathological effects and set of healthy fibers was tested on simulated data. The performances show high level of precision to detect those fibers. We also show how the performances change according to the regularization parameter and the diffusion metrics used to analyze the fiber-bundle. As ulterior step, we applied our method on CST and SLF of two MS patients showing how the fibers affected by the pathological event pass through WM regions affected by real damage. We exploited partially NTF, since we focus our attention to the differentiation of fibers within the bundle. In the future we plan to improve our method in order to increase the performance in terms of recall. Moreover, we plan to exploit also the cross-sectional component (C^*) extracted from the NCPD. The idea is to give more complete information about the region along the fiber-bundle affected by the presence of MS. Moreover, we will extend our method in order to analyze longitudinal data, more in detail, we will increase the order of our tensor to analyze data acquired at different time points. The goal is to underline how a specific WM fiber-bundle is affected longitudinally by the presence of pathologic phenomena.

Acknowledgement. This research was supported by ERC Advanced Grant, #339804 BIOTENSORS and EU MC ITN TRANSACT 2012 #316679.

References

1. Arthur, D., Vassilvitskii, S.: k-means++: The advantages of careful seeding. In: Proceedings of the Eighteenth Annual ACM-SIAM Symposium on Discrete Algorithms, pp. 1027–1035 (2007)
2. Cichocki, A., Zdunek, R., Phan, A.H., Amari, S.I.: Nonnegative Matrix and Tensor Factorizations: Applications to Exploratory Multi-way Data Analysis and Blind Source Separation. Wiley, Chichester (2009)

3. Colby, J.B., Soderberg, L., Lebel, C., Dinov, I.D., Thompson, P.M., Sowell, E.R.: Along-tract statistics allow for enhanced tractography analysis. Neuroimage **59**(4), 3227–3242 (2012)
4. Halandur Nagaraja, B., Sima, D., Sauwen, N., Himmelreich, U., De Lathauwer, L., Van Huffel, S.: Tensor based tumor tissue type differentiation using magnetic resonance spectroscopic imaging. In: Annual International Conference of the IEEE, EMBC, pp. 7003–7006 (2015)
5. Hua, K., Zhang, J., Wakana, S., Jiang, H., Li, X., Reich, D.S., Calabresi, P.A., Pekar, J.J., van Zijl, P.C.M., Mori, S.: Tract probability maps in stereotaxic spaces: analyses of white matter anatomy and tract-specific quantification. Neuroimage **39**(1), 336–347 (2008)
6. MacQueen, J.: Some methods for classification and analysis of multivariate observations. In: Proceedings of the Fifth Berkeley Symposium on Mathematical Statistics and Probability, vol. 1, pp. 281–297 (1967)
7. Mårtensson, J., Nilsson, M., Ståhlberg, F., Sundgren, P.C., Nilsson, C., van Westen, D., Larsson, E.-M., Lätt, J.: Spatial analysis of diffusion tensor tractography statistics along the inferior fronto-occipital fasciculus with application in progressive supranuclear palsy. MAGMA **26**(6), 527–537 (2013)
8. Sorber, L., Van Barel, M., De Lathauwer, L.: Tensorlab v2.0, January 2014
9. Sorber, L., Van Barel, M., De Lathauwer, L.: Structured data fusion. Sel. Top. Sig. Process. **9**(4), 586–600 (2015)
10. Stamile, C., Kocevar, G., Cotton, F., Durand-Dubief, F., Hannoun, S., Frindel, C., Rousseau, D., Sappey-Marinier, D.: Detection of longitudinal dti changes in multiple sclerosis patients based on sensitive WM fiber modeling. In: ISMRM, May-June 2015, Toronto, Canada (2015)
11. Stamile, C., Kocevar, G., Cotton, F., Durand-Dubief, F., Hannoun, S., Frindel, C., Rousseau, D., Sappey-Marinier, D.: A longitudinal model for variations detection in white matter fiber-bundles. In: IWSSIP, pp. 57–60 (2015)
12. Tournier, J.D., Calamante, F., Connelly, A.: MRtrix: diffusion tractography in crossing fiber regions. Int. J. Imaging Syst. Technol. **22**, 53–66 (2012)
13. Varentsova, A., Zhang, S., Arfanakis, K.: Development of a high angular resolution diffusion imaging human brain template. Neuroimage **91**, 177–186 (2014)
14. Yeatman, J.D., Dougherty, R.F., Myall, N.J., Wandell, B.A., Feldman, H.M.: Tract profiles of white matter properties: automating fiber-tract quantification. PLoS One **7**(11), e49790 (2012)
15. Zhang, H., Yushkevich, P.A., Alexander, D.C., Gee, J.C.: Deformable registration of diffusion tensor MR images with explicit orientation optimization. Med. Image Anal. **10**(5), 764–785 (2006)
16. Zink, R., Hunyadi, B., Van Huffel, S., De Vos, M.: Tensor-based classification of auditory mobile BCI without subject-specific calibration phase. J. Neural Eng. **13**(2), 026005 (2016)